1 **Performance and emissions study of diesel and waste biodiesel blends**

2 **with nanosized CZA2 of high oxygen storage capacity**

3 **P. Pimenidou[1*], N. Shanmugapriya[2], N. Shah[3]**

4 [1] School of Engineering, University of Bradford, West Yorkshire BD7 1DP, UK

5 [2] Department of Mechanical Engineering, Siddaganga Institute of Technology,

6 Tumkur-572103. Karnataka, India

7 [3] Built Environment Research Institute, University of Ulster, Newtonabbey, Northern

8 Ireland, BT37 0QB, UK

9

10

11 **Abstract**

12 In this work, the effect of the nanosized CZA2 (cerium-zirconium-aluminium) on the

13 performance and emissions in a two- cylinder indirect injection (IDI) diesel engine,

14 was studied. CZA2 was dispersed in diesel (D100) and waste cooking oil and tallow

15 origin biodiesel-diesel blends (B10, B20, B30) and tested at different engine loads

16 and constant speed. The nanocatalyst (CZA2) increased the brake specific fuel

17 consumption (BSFC) and decreased the brake thermal efficiency (BTE, %) of all

18 tested fuels, at all loads, except B20 at the lowest load. CZA2 reduced nitrogen oxides

19 (NOx) from D100 at low and high engine loads, as well as carbon monoxide (CO)

20 and unburned hydrocarbons (HC) at medium and high tested loads. The dispersion of

21 CZA2 promoted the combustion of the biodiesel blends by almost eliminating HC

22 while reducing NOx and CO emissions at various loads. Thermogravimetric analysis

23 (TGA) coupled with Attenuated Total Reflectance- Fourier Transform Infrared (ATR-

24 FTIR) spectroscopy revealed that the addition of CZA2 in diesel and biodiesel under

25 pyrolysis and oxidation conditions resulted in the presence of saturated species like

26 ketones and final oxidation products such as CO_2, supporting their improved

27 combustion and emissions' reduction in the engine tests.

28 *Keywords:* Redox, waste biodiesel, nanocatalyst, NOx, HC

29

30

1. Introduction

Biodiesel continues to gain attention in combustion and energy conversion technologies due to its sustainability. Especially waste origin biodiesel such as waste cooking oil-sourced biodiesel is deemed the most challenging regarding NOx minimisation. Employment of oxygenated compounds (fatty acid methyl esters) found in biodiesel compared to straight and branched-chain paraffins and aromatic hydrocarbons found in diesel make their combustion more challenging. Therefore, the chemical structure of the biodiesel compounds limits the penetration of biodiesel in the transportation, agriculture and construction sectors. Under lean conditions, biodiesel produces less unburned hydrocarbons (HC) and carbon monoxide (CO), whose presence indicates incomplete combustion, hence insufficient utilisation of the fuel's stored energy expressed by its calorific value. Key challenges in biodiesel combustion are significant emissions production as nitrogen oxides (NOx), a harmful pollutant to humans and the environment. Biodiesel of various origins and similar oxygen content gives different physicochemical properties and produces dissimilar NOx emissions [1] attributed to the structure and unsaturation of the fuel's constituent compounds. Therefore, it is the structure and degree of unsaturation of fatty acids from virgin, waste, plant oils and animal fats either resulting in increased [2-12] or decreased NOx emissions [13-15]. NOx formation is dependent on oxygen concentration relevant to the fuel mixed, combustion temperature and effective volume of the combustion zone according to the Zeldovich mechanism. Higher NOx is noted at high pressure and temperature as in high and full load conditions, as well with a higher rate of combustion leading to higher combustion temperature [9]. Additionally, NOx can be produced during the combustion process at the flame front by CH_2, CH radicals reacting with N_2 via the Fenimore mechanism [16].

Different types of biodiesel-diesel blends compared to diesel show increased brake specific fuel consumption (BSFC) [17-20] in direct injection (DI), compressed ignition engines (CIE) and the less studied indirect injection (IDI) engines [5, 21].

Different approaches have been examined to minimising emissions due to the incomplete combustion of biodiesel-diesel blends. Some of these approaches include the use of additives such as organic peroxides [22] and antioxidants, to aid the limited physicochemical properties of biofuels affected by their chemical composition [16, 23]. Alkaline earth, post-transition metals, metalloids, lanthanides particles and their

1   oxides of a few microns have been tested to enhancing the performance and

2   combustion of biodiesel in diesel engines.

3   Catalytic combustion has already been applied to reduce NOx emissions below

4     $1500^{o}C$ in furnace burners and gas turbine engine combustors. However, catalytic

5   combustion is minorly examined in the transportation sector due to the additional

6   mass, bulk catalysts can add to the system [24-26]. Today, this disadvantage is

7   overcome by the progress in nanoscience and nanotechnology to formulate nanosized

8   catalysts whose enhanced catalytic activity requires small amounts. Emissions' post-

9   treatment by three-way catalysts (TWCs) utilises platinum-rhodium (Pt/ Rh) blends in

10   the reduction of NOx and combined platinum-palladium (Pt/ Pd) to oxidise CO,

11   unburned HC at the exhaust. Cerium oxide mixed with zirconium oxide in TWCs

12   store excess oxygen under fuel-lean conditions and release oxygen under fuel rich

13   conditions [27-28]. Bulk cerium oxide (CeO_2) as a coating in ICEs for enhancing

14   combustion, is reported as early as 1926 [24]. Throughout the 60s, 70s and 80s,

15   modified cerium oxide is reported to boost fuel burning rates while minimising

16   unburned HC emissions from gasoline and diesel engines [24]. Oxygen storage

17   capacity (OSC) of cerium, zirconium (Zr) and aluminium (Al) mixed oxides are

18   reported for hydrocarbons oxidation of combustion [29, 30]. Ce-Zr oxides promote

19   thermal and reduction- oxidation (redox) behaviour of the material and increase their

20   OSC [27, 31].

21   In this work, we study the effect of a ternary nano-catalyst, $Ce_{0.6}Zr_{0.2}Al_{0.26}O_2$ (CZA2)

22   [32] on IDI engine performance indicators and emissions from diesel only (D100) and

23   waste cooking oil and tallow origin biodiesel- diesel blends (B10, B20, B30). Loss of

24   oxygen from CZA2 and reduction of Ce^{4+} to Ce^{3+} increases its thermal expansion

25   coefficient by 11.9% in the temperature region of $600-1000^{o}C$ compared to that of

26    $200-600^{o}C$ [33]. Therefore, thermal stability under combustion conditions is

27   increased, which potentially further supports enhanced catalytic combustion of the

28   tested fuels by CZA2. All tested fuels are analysed by thermogravimetric analysis

29   (TGA) coupled with Attenuated Total Reflectance-Fourier transform infrared (ATR-

30   FTIR) spectroscopy, under inert (pyrolysis) and oxidative (ignition) conditions

31   relative to their performance and emissions in the IDI engine tests.

32

33

34

1

2. Experimental

2.1 Nano-catalysts and fuel blends

Nanosized CZA2 ($Ce_{0.6}Zr_{0.2}Al_{0.26}O_2$, 4.7 nm $\pm$ 0.7 nm) catalysts were produced by the sol-gel method. The method of synthesis, characterisation, initial optimisation, stability and reduction-oxidation capacity were described in previous work [33]. Doping with ZrO_2 and Al_2O_3 overcame inherent limitation of CeO_2 like, low thermal stability and high redox temperature. Additionally, anti-sintering characteristics of Al_2O_3 helped to avoid the particles' agglomeration. CZA2 exhibited high oxygen storage capacity (OSC) and coefficient of thermal expansion (CTE) [33].

Commercial diesel (D100), biodiesel (B100) and 10, 20 and 30% by volume biodiesel in diesel blends, B10, B20 and B30 respectively were tested. Biodiesel originated from waste cooking oil and tallow at a ratio of 60:40 by weight (Green Biofuels Ireland). Homogeneity of blends and uniform dispersion of 0.06 wt% CZA2 in all fuels were ensured with the aid of a magnetic stirrer (IKA C-Mag, model: HS7) for two hours before testing. The relative stability of the nanofuel was observed to be 100 % for the period of 2 hrs. All blends with CZA2 were continuously stirred to maintain suspension throughout the engine feeding. More than 92% relative stability gave sufficient dispersion for the fuel use till 18 hours from its preparation.

2.2 TGA- FTIR

Thermal degradation (pyrolysis) and oxidation (ignition conditions) of the above-described fuels were carried out using a Mettler Toledo TGA/SDTA 851e, with temperature accuracy $\pm0.5°C$, equipped with an alumina pan. All samples were heated under a constant dynamic linear rate of $10°C/$ min, in a 50 $cm^3/$ min nitrogen flow for thermal degradation. The same volumetric flow rate under air from 25 to 600°C was employed. Attenuated Total Reflectance- Fourier Transform Infrared (ATR- FTIR) spectroscopy was carried out on a NEXUS ATR, Thermo Nicolet Spectrometer, in the range of 4000-400 cm^{-1} with a resolution of 4 cm^{-1}. The interval of time between spectra was 60 s.

1

2.3 Characterisation of fuels

Kinematic viscosity was determined in a thermal bath at 40°C by using an Ubbelohde viscometer (PAC (Herzog) Multi Range Viskosimeter HVM 472) according to EN ISO 3104.

Analysis of the inorganic elements was conducted according to EN 14538. Samples of all fuel blends were analysed by PE2400 CHN Elemental Analyser (Perkin Elmer) for carbon, hydrogen, sulphur and nitrogen content. K and Na were determined by inductively coupled plasma mass spectrometry (ICP MS; Varian 820) according to EN 14108/ 14109 and EN 14538 respectively. Ca and Si were determined by inductively coupled plasma optical emission spectrometry (ICP OES; Varian "Vista pro") (EN 14538). Biodiesel samples were diluted in kerosene solvent only, without any other further pre-treatment. Water content was determined using coulometric Karl Fisher titration (Metrohm, KF Coulometer 756) (DIN EN ISO 12937). Gross calorific values were determined using a combustion calorimeter (C 2000- IKA) (DIN 51900).

2.4 Indirect injection engine (IDI) set-up and experimental procedure

All fuels were tested in a four stroke LDW 702 M (FOCS series, Lombardini Group) indirect injection (IDI) engine. The main parameters of the engine are given in Table 1. A schematic diagram of the engine test rig is shown in Figure 1. A net weighted glass cylinder and a digital scale were used to measure the mass of fuel used and a stopwatch to measure the duration of fuel consumption per experiment.

A set of transmitters sent the values of the operation parameters (rotation speed, torque, fuel weight, cooling water flow rate and engine inlet and outlet temperature, fuel- airflow rate, exhaust temperature) to an automatic data acquisition system and were logged by a runtime type software package (LabVIEW). A hydraulic dynamometer (TD-315v4, STEM ISI Impianti) was used to adjust and measure variable engine load (torque) conditions and speed (max operating speed 7000 rpm for dyno rpm f) respectively. Engine load was measured by an electronic load cell with a panel-type instrument for torque measurement range 0÷263 N m. Air was monitored by a fixed choke nozzle (-40÷0 mbar for combustion air flow rate measurement).

1 The engine was warmed up for 30 min with diesel for the biodiesel blends

2 experiments. Each target load was reached with adjustments of speed and torque. The

3 torque was measured with the help of moment arm.

4 The experiments were conducted at variable loads (based on torque) and constant

5 speed of the shaft of 3600 rpm at steady state conditions resulting in small mechanical

6 losses. These conditions would lead to conclusions on the effect all tested fuels and

7 CZA2 had on the engine's performance characteristics and emissions. A four gases

8 emissions analyser (AUTOplus automotive) measured nitrogen oxides (NOx, ppm),

9 carbon monoxide (CO, %), carbon dioxide (CO_2, %) and total unburned hydrocarbons

10 (HC, ppm) at the exhaust. The analyser had an accuracy of ± 5% of reading. At each

11 load, the engine was stabilised for 4 min, and then the measurement parameters per

12 tested blend were recorded. All fuels were tested three times under steady state

13 conditions, and the results were averaged to decrease the uncertainty.

14 Performance indicators such as brake power (BP, kW), brake specific fuel

15 consumption (BSFC, kg/ (kW·s)) and % of brake thermal efficiency (BTE,%) of all

16 fuels were calculated as follows:

17 $$BP\ (kW) = \frac{2 \cdot \pi \cdot RPM \cdot \tau}{60 \cdot 1,000} \qquad \text{Eq. (1)}$$

18 where τ is the brake toque (Nm),

19 $$BSFC = \frac{\dot{m}_f\ (\frac{kg}{s})}{BP\ (kW)} \qquad \text{Eq. (2)}$$

20 where $\dot{m}_f$, fuel consumption rate (kg/s),

21 $$BTE,\% = \frac{3,600}{BSFC \cdot LHV} \cdot 100 \qquad \text{Eq. (3).}$$

22

23

24 *2.5 Engine performance and emissions statistical analysis*

25 Engine performance and emissions statistical analysis were conducted on the

26 calculated engine performance parameters, aka of the average BSFC, BTE and

27 emissions of all fuels. The two-way analysis of the variance (ANOVA) with Fischer's

28 least significance difference (LSD) post-hoc analysis [34] were applied to show the

29 level of significance of the load, the addition of CZA2 in each fuel and the synergy of

30 the addition of CZA2 and the load, by using SPSS (v24) software (IBM). The *F*-ratio

31 is the ratio of the two mean square values, comparing each variation source, and the

32 *p*-value determined the statistical level of significance. When a *p*-value was less than

1   or equal to 0.05 the mean values of BSFC, BTE (%) and emissions of all fuels would

2   indicate the different performance and emissions of each fuel. A p-value greater than

3   0.05 would show statistical non-significance.

4

5

6   ### 3. Results and discussion

7   *3.1 TGA-FTIR analysis*

8   Figures 2. (a) and (b) showed single step curves of pyrolysis and oxidation

9   respectively for all tested fuels. One-step mass remaining curves of all tested fuels

10   suggested that operational engine problems, such as slow and inhibited multi-step

11   burning under pyrolysis and ignition conditions, would not be met [35]. Two

12   distinctive phases of decomposition were identified: (i) low- ($< 230^{o}$C) and (ii) high-

13   temperature ($> 230^{o}$C). Pyrolysis of D100 and B100 started at 60°C and 50°C

14   respectively while the volatilisation of pure biodiesel (B100) started at 120°C, a

15   higher temperature than the rest of the tested fuels as seen in Fig. 2 (a1). Pyrolysis of

16   D100 finished at 290°C, an earlier temperature compared to the remainder of the

17   tested fuels (Fig. 2. (a1)). B100 was fully decomposed by 310°C, which was attributed

18   to more unsaturated bonds present compared to diesel. Lower volatility linked to

19   higher intramolecular forces of B100 giving to the fuel higher viscosity. The

20   volatilisation of B100-CZA2 started at 140°C, a temperature 20°C higher compared to

21   B100, and the pyrolysis of D100-CZA2 was initiated at 65°C. B100-CZA2 and D100-

22   CZA2 pyrolysis ended at around 270°C and 300°C respectively. Overall, dispersion of

23   CZA2 reduced the temperature range of pyrolysis of D100 by postponing its initial

24   and advancing the final pyrolysis to higher temperatures and lower temperatures

25   respectively compared to the corresponding tests in the absence of CZA2. The initial

26   and final pyrolysis temperatures of biodiesel and biodiesel blends with CZA2 were

27   raised. Such an outcome was further reflected in the increased D100-CZA2 and

28   decreased B100-CZA2 mass losses in Fig. 2. (a2) compared to D100 and B100

29   pyrolysis in the low-temperature region in Fig. 2. (a1). The presence of CZA2 in the

30   low-temperature region increased mass losses of D100 from 66.81% (33.19% residual

31   mass) to 77.82% (22.18% residual mass) and marginally increased the mass losses of

32   B100 from 32.16% (67.84% residual mass) to 32.68% (67.32% residual mass)

33   respectively. All biodiesel blends followed the pattern of D100 pyrolysis in the low-

34   temperature region; the biodiesel content dominated the pyrolysis of B30 in the high

1　temperature region (Fig. 2. (a1)). Pyrolysis of all biodiesel blends with CZA2

2　demonstrated a unique catalytic thermal cracking identity, incomparable to D100-

3　CZA2 and B100-CZA2 at all temperatures except B30-CZA2 which pyrolysed

4　similarly to B100-CZA2 in the high-temperature region.

5　Under ignition conditions, decomposition of D100 and B100 concluded at 280 and

6　310°C respectively (Fig. 2. (b1)). All tested biodiesel blends in the absence and

7　presence of CZA2 were fully oxidised by approximately 300°C (Fig. 2. (b2)). Mass

8　losses of D100 and B100 at 230°C were 70.02% (29.98% residual mass) and 23.32%

9　(76.68% residual mass) under ignition conditions (Fig. 2. (b1)), compared to 66.81%

10　(33.19% residual mass) and 32.16% (67.84% residual mass) respectively under

11　pyrolysis conditions (Fig. 2. (a1)). Mass losses of D100-CZA2 and B100-CZA2 at

12　230°C were 70.02% (29.98% residual mass) and 23.32% (76.68% residual mass)

13　under ignition conditions (Fig. 2. (b2)), compared to 77.82% (22.18% residual mass)

14　and 32.68% (67.32% residual mass) under pyrolysis conditions (Fig. 2. (a2)). The

15　oxidation curves of all biodiesel blends showed a similar rate of consumption within

16　the same temperatures to those of D100 rather than B100 (Fig. 2. (b1)). Dispersion of

17　CZA2 in all biodiesel blends under ignition conditions led to their almost identical

18　behaviour by shifting the oxidation of these blends to higher temperatures than in the

19　absence of CZA2. Dispersion of CZA2 under ignition conditions gave to all biodiesel

20　blends a different behaviour to D100-CZA2 and B100-CZA2.

21　FTIR spectra were obtained simultaneously to the TGA data to gain insight on the

22　thermal decomposition and oxidation of the tested fuels in the absence and presence

23　of CZA2 (Fig. 3. (a) and (b)). The mid- IR spectral region (4000- 400 cm^{-1}) showed in

24　the past some incomparable peaks between biodiesel and diesel. Here, FTIR spectra

25　of all TGA experiments at 150°C were chosen since CZA2 oxygen transfer was

26　initiated at this temperature [33].

27　CZA2 dispersion in D100 under pyrolysis conditions resulted in the additional peaks

28　of C=O assigned to CO_2 (2343 and 2283 cm^{-1}), C≡O attributed to CO (2100 cm^{-1}),

29　C=O attributed to ketones (1740 cm^{-1}) (Fig. 3. (a2)). D100-CZA2 under ignition

30　conditions produced less pronounced peaks of CH_2 (1450 cm^{-1}), C-H bending (1380

31　cm^{-1}), CO_2, CO and ketones (Fig. 3. (b2)) compared to D100-CZA2 under pyrolysis

32　conditions and D100 under ignition conditions (Fig. 3. (b1)). Pyrolysis of B100 at

33　150°C produced the same but much weaker absorption peaks than D100. Dispersion

34　of CZA2 into B100 produced significant bands at 2954 and 2854 cm^{-1} by sp^{3}

1 hybridised C-H stretch (Fig. 3. (a4)). The absence of the band attributed to CO was

2 noted for the same fuel, and stronger absorption peaks were recorded due to ketones

3 and CH_2, CH bending compared to D100-CZA2 under pyrolysis (Fig. 3. (a2)).

4 Oxidation of B100 resulted in weaker bands absorption (Fig. 3. (b3)) than B100-

5 CZA2 (Fig. 3.(b4)). Ketones absorption band was more pronounced for B100-CZA2

6 (Fig. 3. (b4)) than D100-CZA2 under ignition conditions (Fig. 3. (b2)).

7 Wexler [36] found that esters in the presence of metals such as cerium and zirconium

8 could lead to the formation of hydroperoxides, which by oxidation-reduction

9 produced aldehydes and ultimately ketones. Phenol could inhibit further oxidation

10 reactions by reacting with the free peroxy radical. In the same work [36] the

11 formation of lower aldehydes was considered a product of secondary oxidation (chain

12 propagation) of fatty acid esters from unsaturated ester peroxides (ROOH) which

13 were produced from the primary oxidation of esters. In particular, metals acting as

14 oxygen carriers could oxidise esters through different steps in forming
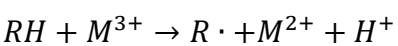
15 hydroperoxides by:

16 (1) attack of the oxygen atom to an activated methylene group and the produced alkyl
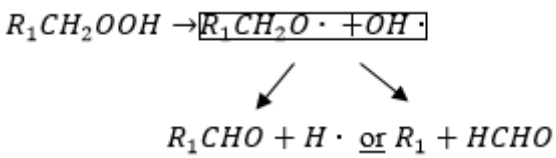
17 radical

$$M - O - O \cdot \xrightarrow{-CH_2CH=CH-} M - O - O - H + -\dot{C}HCH = CH -$$
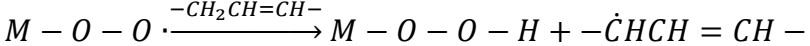
18 (2) direct attack of a metal ion to an olefinic double bond

$$RCH = CH_2 + M^{3+} \rightarrow RCH = CH_2^+ + M^{2+}$$
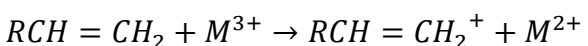
19 (3) direct attack of a metal ion to a saturated bond

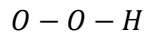$$RH + M^{3+} \rightarrow R \cdot + M^{2+} + H^+$$

20 The radical produced by all possible mechanisms could react with oxygen to produce

21 a hydroperoxide by chain propagation. The hydroperoxides could then either

22 decompose to produce an alkoxy and OH radical or break down to produce lower
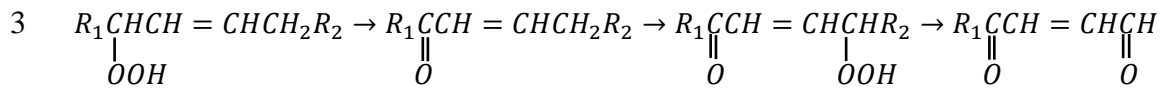
23 aldehydes:

$$R_1CH_2OOH \rightarrow \boxed{R_1CH_2O \cdot + OH \cdot}$$

$$R_1CHO + H \cdot \text{ or } R_1 + HCHO$$

24

25 Further oxidation of aldehydes led to the formation of acids, including some

26 unsaturated acids, and CO [36]. Oxidative attack of acid radicals resulted in methyl-

27 ketones and CO_2:

28 $R_1CH_2CH_2COOR_2 \xrightarrow{O_2} R_1\dot{C}HCH_2COOR_2 \rightarrow R_1COCH_2COOR_2 \rightarrow R_1COCH_3 + CO_2$
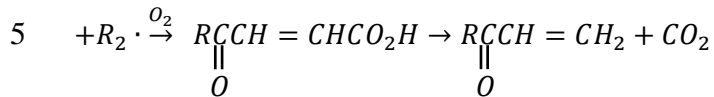
$$O - O - H$$
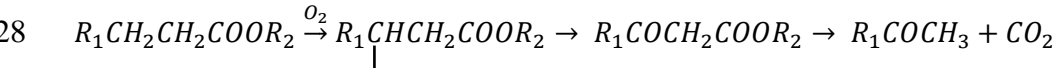
1   Methyl- ketones could also be produced by the decomposition of vinyl ketones

2   formed by the oxidation of the double bond:

3    $R_1 \underset{\underset{OOH}{|}}{CH}CH = CHCH_2R_2 \rightarrow R_1 \underset{\underset{O}{\parallel}}{C}CH = CHCH_2R_2 \rightarrow R_1 \underset{\underset{O}{\parallel}}{C}CH = CHCHR_2 \rightarrow R_1 \underset{\underset{O}{\parallel}}{C}CH = CH\underset{\underset{O}{\parallel}}{C}H$
     (with OOH under the third group)

4

5    $+R_2 \cdot \xrightarrow{O_2} R\underset{\underset{O}{\parallel}}{C}CH = CHCO_2H \rightarrow R\underset{\underset{O}{\parallel}}{C}CH = CH_2 + CO_2$

6   Formation of these ketones and carboxylic acids could also occur during thermal

7   cracking between 245- 260°C.

8

9

10   *3.2 Engine performance*

11   The addition of biodiesel into diesel decreased BP to a small degree at 21 and 25 Nm

12   whereas it marginally increased BP at lower loads. The dispersion of CZA2 decreased

13   BP on average by 0.2- 5% for all biodiesel blends (Fig. 4) and by -4- 1.3% for D100,

14   from low to high load conditions.

15   All biodiesel blends exhibited lower BTE than diesel at all loads. Lower BTE of the

16   biodiesel blends compared to diesel fuel is mainly due to high viscosity and low

17   heating value of the blend (Table 2). The BTE of D100-CZA2 declined at all load

18   conditions compared to D100 credited to the oxygenated compounds produced under

19   pyrolysis and ignition conditions relevant to the FTIR analysis in paragraph 3.1. Table

20   4 shows the results of ANOVA and LSD along with the *F* ratio of the BSFC and BTE

21   for each fuel and the associated p-value. The statistical analysis affirmed the

22   significant effect of load and addition of CZA2 on the reduction of BTE of diesel

23   (Table 4). The BTE was reduced by dispersion of CZA2 in all biodiesel blends and at

24   all loads. These results indicated that the combustion of all fuels with the CZA2 at all

25   loads was almost complete, despite that at the high load conditions the duration of

26   combustion was expected to decrease. All biodiesel blends' BTE reduction was more

27   pronounced at high than at low loads. The load had a substantial impact on the

28   decrease in BTE as seen in Table 4. Additionally, the dispersion of CZA2 became

29   more significant by increasing the biodiesel content in the fuel.

30   All blends with CZA2 under the majority of applied loads exhibited the mirroring

31   effect of an increased BSFC against a decreased BTE as expected. The brake specific

1 fuel consumption (BSFC) increased with the addition of biodiesel into diesel at all

2 loads (Fig. 5), reflecting on the decrease of the BTE at the same loads (Fig. 6). The

3 BSFC of the same blends decreased with increasing load due to the increasing BP at

4 higher loads [17]. Here, the decreasing trend of BSFC (Fig. 5) with adding biodiesel

5 in diesel at higher loads reflected on the increasing BTE (Fig. 6), similarly to earlier

6 performance studies at a constant speed and variable loads [20, 21, 37]. Such an effect

7 could be assigned to less fuel needed to operate the engine at high loads due to

8 minimisation of heat losses compensating for the increase in brake power (BP).

9 Furthermore, BSFC was calculated on a mass basis while the heating value of D100

10 was 2-3.8% higher than those of B10, B20 and B30 (Table 3). The increase in BSFC

11 when using D100-CZA2 on an average by approximately 16% compared to D100 at

12 all loads, suggested faster combustion due to catalysis that led to additional fuel

13 consumption per power produced, compared to the D100 engine tests. The

14 pronounced effect of the addition of CZA2 and the various loads on the BSFC when

15 D100 was tested was confirmed by the statistical analysis (Table 4). The BSFC was

16 amplified by B10-CZA2 versus B10 mainly at the high load conditions, between B20-

17 CZA2 and B20 from medium to high loads (15, 21 and 25 Nm) and by dispersion of

18 CZA2 in B30 at all loads on average by approximately 12% (Fig. 5; Table 4). These

19 results underlined the different chemistry of the fuels during catalytic combustion

20 based on the groups of compounds identified in FTIR representing the fuel

21 compounds in the fuel rich and lean zones. As it was illustrated by the TGA-FTIR

22 study of diesel and biodiesel, the routes towards catalytic combustion of diesel and

23 biodiesel blends were expected to be different. The various mechanisms of pyrolysis

24 and oxidation could have led to intermediate products which would have given rise to

25 different catalytic combustion steps and whose complexity was apparent through the

26 various correlations of BSFC and BTE when CZA2 was dispersed in the tested fuels.

27

28

29 *3.3 Engine emissions characteristics*

30 *3.3.1 HC emissions*

31 Diesel produced more unburned HC than all biodiesel blends in the engine tests at the

32 high and full load conditions (Fig. 7.(a)), a well- established phenomenon as per

33 previous studies [1, 8, 20, 38] due to the higher oxygen content of biodiesel (Table 3).

34 The dispersion of CZA2 reduced the HC emissions from D100 at the high and full

1   loads appreciably (Fig. 7. (a)), underlining the benefit catalytic combustion offers as

2   well as the advantage of dispersion of oxygen released from CZA2. More specifically,

3   in the FTIR spectrum of the D100-CZA2 profile the peaks of CO, CO_2 and ketones

4   identified, which were not found in the FTIR profile of D100 under pyrolysis

5   conditions, affirmed an easier combustible mixture here evidenced by the reduced HC

6   emissions during the catalytic combustion of D100. The profound effect of load, the

7   addition of CZA2 and the synergy of load and addition of CZA2 on HC emissions

8   from D100 was affirmed by the statistical analysis (Table 4). All biodiesel blends

9   with CZA2 blends had an overall significant effect on diminishing the presence of HC

10 found at the exhaust from the full load engine tests (Fig. 7. (a)). The lowest HC

11 emissions resulted in 0.06 ppm with B30 at 10 Nm, 0.03 ppm with B10-CZA-2 at 5

12 Nm, 0.05 ppm with B30-CZA2 at 21 Nm, 0.03 ppm with B30-CZA2 at 15 and 25

13 Nm. Unburned HC emissions were linked in the past to misfire in the locally lean

14 region or rich region. Here the redox property of ceria enabled the release of oxygen

15 in the fuel rich zone and absorbed oxygen from the lean fuel zone, which could assist

16 combustion to reach completion. An overall decreasing trend of HC emissions

17 decrease was identified with less biodiesel blended in diesel with CZA2 in the low

18 load (B10-CZA2< B20-CZA2< B30-CZA2 (Fig. 7.(a)). This outcome could be traced

19 in the shift of the decomposition of B10-, B20- and B30- CZA2 towards the one of

20 B100-CZA2 at high temperatures under ignition conditions (Fig. 2. (b2)), which gave

21 a prominent release of oxygenated compounds, such as ketones, in the FTIR (Fig. 3.

22 (b4) further justified the minimisation of the HC emissions.

23 Furthermore, the statistical analysis confirmed the profound effect CZA2 addition and

24 load had on HC reduction when B10 was used (Table 4). The use of CZA2, load and

25 synergy between the catalyst and load had a significant impact on the HC emissions

26 from B20. From Table 4, the reduction of HC emissions with the use of B30-CZA2

27 compared to B30 was attributed mainly to the effect of the load and synergy of the

28 catalyst with load.

29

30 *3.3.2 Carbon oxides*

31 Carbon monoxide (CO) appeared reduced at all high loads by the addition of biodiesel

32 compared to D100 except at the lowest load (Fig. 7(b)) contrary to earlier reports

33 where CO emissions of same biodiesel blends appeared larger compared to those of

34 diesel [39]. The addition of CZA2 in D100 reduced CO emissions at high loads (Fig.

7(b)) affected by the addition of CZA2 (Table 4). CZA2 addition to B10 and B30 reduced CO emissions only at the middle loads and to B20 in the low loads (Fig. 7(b)). The effect of the load was pronounced for the reduction of CO emissions for all biodiesel blends with CZA2, while the impact of CZA2 addition with the load on CO production was significant for B20 and B30 (Table 4).

Carbon dioxide (CO_2) emissions from the catalytic combustion of all biodiesel blends increased compared to D100 at the high and full load conditions (Fig. 7(c)). The statistical analysis also indicated the significant impact CZA2, load and both CZA2 and load had on the increase of CO_2 from D100 (Table 4). The decrease of CO by the addition of CZA2 into biodiesel blends was not accompanied by the same extent of CO_2 emissions decrease. Such an outcome could signify two phenomena, which occurred in parallel and consecutively: (i) the enhancement of combustion of biodiesel blends directly to CO and CO_2, (ii) oxidation of produced CO to CO_2 by an increase of the overall CO_2 emitted. The different possible mechanisms of aldehydes and ketones formation via peroxides production were discussed in paragraph 3.1. Organic peroxides indicated to catalytically reduce emissions possibly through the formation of ketones [22]. Earlier research also showed that the catalytic oxidation of aldehydes increased the rate of the termination step, through an increased peroxy formation resulting in enhanced CO_2 production [40]. Therefore, CZA2 promoted here the termination mechanism of combustion in the direction of CO_2 formation by contributing towards oxygen delivery and producing more CO and CO_2 through the mechanisms described in paragraph 3.1, therefore, reducing HC emissions. Increased oxygen contact time with the tested fuels during combustion also reflected on the marginal increase in the BP of all biodiesel blends with CZA2, consequently utilising the energy of the fuels. The reduction of CO_2 emissions by addition of biodiesel content in diesel with CZA2 was significant regarding load for B10, load and the synergy of CZA2 and load for B20 and CZA2, load and combination of CZA2 and load for B30.

3.3.3 Oxides of nitrogen

Our results showed higher NOx emissions from D100 compared to B10, B20 and B30 at all loads except at full load (Fig. 7(d)) similarly to previous work [5, 9]. Blends with higher content in biodiesel produced less NOx at the low loads and more NOx than D100 at the full load. NOx production followed an increasing trend from low to

1 high and full load conditions due to increasing adiabatic flames temperatures allowing

2 higher combustion temperature and time at full load while cooling was not sufficient

3 [5, 41].

4 D100-CZA2 minimised NOx emissions compared to D100 on an average by 8.04% at

5 all conditions. D100-CZA2 had the lowest NOx emissions compared to all biodiesel

6 blends-CZA2 at the low loads. The significant effect of load on the NOx emissions

7 between D100 and D100/CZA2 is shown in Table 4. The addition of organo-mono-

8 metallic oxides to diesel showed enhancement of NOx emissions and reduction of the

9 specific consumption of fuel [42], whereas here we achieved reduction of NOx and

10 increase of BSFC by the use of CZA2.

11 B10-CZA2 generated slightly lower NOx emissions at 15 and 21 Nm, compared to

12 B10. B20-CZA2 produced less NOx than B20 at all loads, except at the highest load.

13 B30-CZA2 achieved an average reduction of NOx emissions at all loads by 13.34%.

14 FTIR spectra showed earlier that oxidation of biodiesel (unsaturated, oxygenated

15 compounds) with CZA2 produced more noticeable saturated (alkane) and ketone

16 peaks. Earlier research found that fuel with higher content of unsaturated compounds

17 produced more NOx compared to saturated compounds [12]. Therefore, the presence

18 of CZA2 catalysed the fuel blends resulting in their products combustion, which led

19 to reduced NOx emissions (Fig. 7(d)). The minimisation of NOx emissions could be

20 advanced due to a delay in the ignition [22]. It was described earlier that all biodiesel

21 blends with CZA2 under ignition conditions oxidised at a higher temperature than in

22 the absence of CZA2 (Fig. 2. (b2), paragraph 3.1). NOx emissions of both B10-CZA

23 and B20-CZA2 were mainly affected by the load while those from the use of B30-

24 CZA2 by the addition of CZA2, load and the synergy of CZA2 and load (Table 4).

25 The reduced form of CZA2, through absorption of available oxygen during

26 combustion, expected the minimisation of NOx; when this was not possible at

27 extremely high combustion temperatures, a lessened catalytic activity during

28 combustion or fast kinetics of combustion surpassing the rate of the reduction

29 capability of the catalyst was expected. Fast combustion as depicted in the increased

30 BSFC at all loads of B30-CZA2 was expected to cause additional air pumped which

31 would promote oxidation of CO towards CO2 and N2 in the air towards NOx; the

32 latter did not occur. On the contrary, here CZA2, when dispersed in the fuel blends,

33 acted oxidatively and released oxygen by potentially setting the endothermic catalytic

34 combustion of biodiesel-diesel blends dominant at high load conditions. Therefore,

the decrease of both NOx and combustion carbon emissions revealed the simultaneous occurrence of the otherwise antagonistic mechanisms of reducing flames temperature and fast combustion. This effect could be possible through reducing the flame temperature due to the highly endothermic catalytic combustion reactions resulting in the minimised HC emissions (Fig. 7(a)) and hindering NOx formation (Fig. 7(d)). Adiabatic flames temperature was found to be lower when produced by combustion of saturated than of unsaturated molecules [12].

Overall, catalytic combustion of diesel and biodiesel-diesel blends by using CZA2 revealed its valuable oxidative character by promoting the consumption of heat released by combustion of the highly endothermic catalytic reactions and production of intermediate products leading to almost complete combustion with fewer HC emissions and less favourable conditions for NOx formation.

4. Conclusions

This study explored the effect of nanocatalytic combustion with CZA2 on diesel and waste- origin biodiesel-diesel blends performance and emissions from an indirect injection diesel engine under various loads. Our experimental results showed the reduction of the emissions from diesel and B10, B20, B30 when using CZA2.

The presence of CZA2 enhanced the pyrolysis of all investigated fuels in the TGA tests. All biodiesel blends (B10, B20, B30) behaved similarly to D100 at all temperatures under ignition conditions. On the other hand, biodiesel blends behaved similarly to D100 at all temperatures under the pyrolysis conditions with the exception of B30, which thermally decomposed similarly to B100 over 230°C. FTIR under pyrolysis and ignition conditions showed a different distribution of compounds for diesel and biodiesel when dispersing CZA2. In particular, ketone bands were identified via the formation of hydroperoxides, which could have enhanced the combustion in the engine tests. However, definitive results concerning the specific compounds formed by all tested fuels (D100, B10, B20, B30) with CZA2 during combustion in the engine tests could not be established.

Fuel consumption increased for all tested fuels with the dispersion of CZA2, which was attributed to the improved combustion as evidenced by the reduction of the unburned hydrocarbons (HC) and carbon monoxide (CO) emissions from the exhaust. At the same time, the reduced nitrogen oxides (NOx) emissions suggested that CZA2

1 induced a trade-off between the mechanisms of NOx formation and close to complete

2 combustion.

3

4

5

References

[1] F. Wu, J. Wang, W. Chen, S. Shuai A study on emission performance of a diesel engine fueled with five typical methyl ester biodiesels Atmos Environ, 43 (2009), pp. 1481–1485

[2] O. Can Combustion characteristics, performance and exhaust emissions of a diesel engine fuelled with waste cooking oil biodiesel mixture Energy Convers Manage, 87 (2014), pp. 676- 686

[3] A. C. Hansen, M. R. Gratton, W. Yuan Diesel engine performance and NO_X emissions from oxygenated biofuels and blends with diesel fuel Trans ASABE, 49 (2006), pp. 589–595

[4] J. T. Song, C. H. Zhang An experimental study on the performance and exhaust emissions of a diesel engine fuelled with soybean oil methyl ester P I Mech Eng D-J Aut, 222 (2008), pp. 2487–2496

[5] N. Usta Use of tobacco seed oil methyl ester in a turbocharged indirect injection diesel engine Biomass Bioenerg, 28 (2005), pp. 77–86

[6] N. Usta, E. Öztürk, Ö Can, E.S. Conkur, S. Nas, A. H. Con, A. C. Can, M. Topcu Combustion of biodiesel fuel produced from hazelnut soapstock/ waste sunflower oil mixture in a diesel engine Energ Convers Manage, 46 (2005), pp. 741–755

[7] L. Zhu, W. Zhang, W. Liu, Z. Huang Experimental study on particulate and NO_X emissions of a diesel engine fueled with ultra low sulfur diesel, RME-diesel blends and PME-diesel blends Sci Total Environ, 408 (2010), pp. 1050–1058

[8] S. Godiganur, C.H.S. Murthy, R. P. Reddy Performance and emission characteristics of a Kirloskar HA394 diesel engine operated on fish oil methyl esters Renew Energ, 35 (2010), pp. 355–359

[9] P. K. Sahoo, L. M. Das, M. K. G. Babu, P. Arora, V. P. Singh, N. R. Kumar Comparative evaluation of performance and emission characteristics of jatropha, karanja and polanga based biodiesel as fuel in a tractor engine Fuel, 88 (2009), pp. 1698–1707

[10] G. Fontaras, G. Karavalakis, M. Kousoulidou, T. Tzamkiozis, L. Ntziachristos, E. Bakeas Effects of biodiesel on passenger car fuel consumption, regulated and non-regulated pollutant emissions over legislated and real-world driving cycles Fuel, 88 (2009), pp. 1608–1617

[11] C. S. Cheung, L. Zhu, Z. Huang Regulated and unregulated emissions from a diesel engine fueled with biodiesel and biodiesel blended with methanol. Atmos Environ 43 (2009), pp. 4865–4872

[12] G. A. Ban-Weiss, J. Chen, B. A. Buchholz, R. W. Dibble A numerical investigation into the anomalous slight NOx increase when burning biodiesel; a new (old) theory Fuel Process Technol, 88 (2007), pp. 659–667

[13] H. Aydin, H. Bayindir Performance and emission analysis of cottonseed oil methyl ester in a diesel engine Renew Energ, 35 (2010), pp. 588–592

[14] S. Kalligeros, F. Zannikos, S. Stournas, E. Lois, G. Anastopoulos, C. Teas, F. Sakellaropoulos An investigation of using biodiesel/ marine diesel blends on the performance of a stationary diesel engine Biomass Bioenerg, 24 (2003), pp. 141–149

[15] R. L. McCormick, M. S. Graboski, T. L. Alleman, A. M. Herring, K. S. Tyson Impact of biodiesel source material and chemical structure on emissions of

criteria pollutants from a heavy-duty engine Environ Sci Technol, 35 (2001), pp. 1742–1747

[16] I.M.R. Fattah, M. H. Hassan, M. A. Kalam, A. E. Atabani, M. J. Abedin Synthetic phenolic antioxidants to biodiesel: path toward NOx reduction of an unmodified indirect injection diesel engine J Clean Prod, 79 (2014), pp. 82- 90

[17] X. Meng, G. Chen, Y. Wang Biodiesel production from waste cooking oil via alkali catalyst and its engine test Fuel Process Technol, 89 (2008), pp. 851- 857

[18] H. Raheman, S.V. Ghadge Performance of compression ignition engine with mahua (Madhuca indica) biodiesel Fuel, 86 (2007), pp. 2568- 2573

[19] D.H. Qi, H. Chen, L.M. Geng, Z. H.Y. Bian Experimental studies on combustion characteristics and performance of a direct injection fueled with biodiesel/ diesel blends Energy Convers Manage, 51(2010), pp. 2985- 2992

[20] S. Puhan, G. Nagarajan, N. Vedaraman, B. V. Ramabramhmam Mahua oil (Madhuca indica oil) derivatives as a renewable fuel for diesel engine systems in India, a performance and emissions comparative study Int J Green Energy, 4 (2007), pp. 89–104

[21] H. Raheman, S.V. Ghadze Performance of diesel engine with biodiesel at varying compression ratio and ignition timing Fuel, 87 (2008), pp. 2659–2666

[22] P. Purusothaman, A. Gurusamy Effect of di tertiary butyl peroxide additive on performance and emission characteristics of biodiesel butanol blends IJERT 3 (2014), 3, pp. 1002- 1007

[23] K. Ryu The characteristics of performance and exhaust emissions of a diesel engine using a biodiesel with antioxidants Bioresource Technol, 101 (2010), pp. S78–S82

[24] R. L. Jones Catalytic combustion effects in internal combustion engines, Combust Sci Technol 129 (1997), pp. 185- 195

[25] T.J. Rychter, R. Saragih, T. Lezanski, S. Wojcicki Catalytic activation of a charge in a prechamber of a SI lean- burn engine Symp Int Combust, 18 (1981), pp. 1815- 1824

[26] R.H. Thring The catalytic engine Platin Met Rev, 24 (1980), pp. 126- 133

[27] J. Kaspar, P. Fornasiero, N. Hickey Automotive catalytic converters: current status and some perspectives Catal Today, 77 (2003), pp. 419- 449

[28] R.J. Farrauto, R.M. Heck Catalytic converters: state of the art and perspectives Catal Today, 51 (1999), pp. 351- 360

[29] W. Liu, M. Flytzani- Stephanopoulos Transition metal- promoted oxidation catalysis by fluorite oxides: A study of CO- oxidation over Cu- CeO_2 Chem Eng J, 64 (1996), pp. 283- 294

[30] A. Trovarelli, C. de Leitenburg, M. Boaro, G. Dolcetti The utilisation of ceria in industrial catalysis Catal Today, 50 (1999), pp. 353- 367

[31] R.G. Rao Influence of metal particles on the reduction properties of ceria- based materials studied by TPR Bull Mater Sci, 22 (1999), pp. 89- 94

[32] N. Shanmugapriya, C. Somayaji, S. Kanagaraj Characterization and optimization of $Ce_{0.6}Zr_{0.4-x}Mn_xO_2$ (x≤0.4) J Nanopart Res, 16 (2014), pp. 2661

[33] N. Shanmugapriya, C. Somayaji, S. Kanagaraj Optimization of $Ce_{0.6}Zr_{0.4-x}Al_{1.3x}O_2$ solid solution based on oxygen storage capacity J Nanopart Res, 16 (2014), pp. 1- 10

[34] Gonzales R. Data analysis for experimental design. The Guilford Press (2009)

[35] C.M. Soares, L.C.V. Itavo, A.M. Dias, E.J. Arruda, A.A.S.T. Delben, S.L. Oliveira, L.C.S. de Oliveira Forage turnip, sunflower, and soybean biodiesel

obtained by ethanol synthesis: Production protocols and thermal behaviour Fuel, 89 (2010), pp. 3725–3729

[36] H. Wexler Polymerisation of drying oils Chem Rev, 64 (1964), pp. 591- 611

[37] M.I. Arbab, H.H. Masjuki, M. Varman, M.A. Kalam, S. Imtenan, H. Sajjad Experimental Investigation of Optimum Blend Ratio of Jatropha, Palm and Coconut Based Biodiesel to Improve Fuel Properties, Engine Performance and Emission Characteristics SAE Tech Pap, 2013-01-2675

[38] M. Zheng, M.C. Mulenga, G.T. Reader, M. Wang, D. S. K. Ting, J. Tjong Biodiesel engine performance and emissions in low temperature combustion Fuel, 87 (2008), pp. 714-722

[39] A. Abu-Jrai, J.A. Yamin, A.H. Al-Muhtaseb, M.A. Hararah Combustion characteristics and engine emissions of a diesel engine fueled with diesel and treated waste cooking oil blends Chem Eng J, 172 (2011), pp. 129–136

[40] D.R. Larkin The role of catalysts in the air oxidation of aliphatic aldehydes J Org Chem, 55 (1990), pp. 1563–1568

[41] M. Lapuerta, O. Armas, R. Ballesteros, J. Fernández Diesel emissions from bio-fuels derived from Spanish potential vegetable oils Fuel, 84 (2005), pp. 773–780

[42] A. Keskin, G. Metin, D. Altiparmak Influence of metallic based fuel additives on performance and exhaust emissions of diesel engine Energy Convers Manage, 52 (2011), pp. 60-65

Table 1. Specification of test engine.

Technical parameters	Technical data
Engine type	4-strokes diesel engine
Number of cylinders	2
Bore	75 mm
Stroke	77.6 mm
Dry weight	66 kg
Compression ratio	22.8 : 1
Displacement	686 cm^3
Injection system	Indirect injection
Aspiration	Normal
Cooling system	Water cooled via heat exchanger
Rated speed	3,600 rpm
Rated power	10.7 kW @ 3600 rpm
Maximum torque	40.5 N m @ 2000 rpm

Table 2. Percentage uncertainties and errors of instruments, measurements and performance indicators

Instrument	Emission	Measuring range	Error
AUTOplus automotive	NOx	0- 15,000 ppm	± 1 ppm
	CO	0- 10% vol	± 0.01%
	CO_2	0- 16% vol	± 0.1 %
	HC	0- 5,000 ppm	± 1 ppm

Measurements	Measuring range	Accuracy
Load monitoring	0- 236 Nm	± 0.2 Nm
Speed measuring	0- 7,000 rpm	± 15 rpm
Fuel consumption (mass)	0- 20,000 g	± 2 g

Table 3. Physical and chemical properties of diesel, diesel- biodiesel blends and biodiesel.

Analysis fuel Standards	D100 EN 590	B10 EN 16734	B20 EN 16709	B30 EN 16709	B100 EN 14214
Kinematic viscosity (mm^2/ s) (@40°C)	2.824	2.957	3.109	3.231	4.535
Test method and limits	EN ISO 3104 2.000- 4.500	EN ISO 3104 2.000- 4.500	EN ISO 3104 2.000- 4.620	EN ISO 3104 2.000- 4.650	EN ISO 3104 3.500- 5.000
Proximate					
Calorific value, upper (MJ/kg)	45.49 DIN 51900- 1 mod.	44.68 DIN 51900- 1 mod.	44.22 DIN 51900- 1 mod.	43.68 DIN 51900- 1 mod.	40.33 DIN 51900- 1 mod.
Test method and limits	No limit	No limit	No limit	No limit	No limit
Calorific value, lower (MJ/kg)	42.62 DIN 51900- 2 mod.	41.75 DIN 51900- 2 mod.	41.61 DIN 51900- 2 mod.	40.96 DIN 51900- 2 mod.	37.67 DIN 51900- 2 mod.
Test method and limits	No limit	No limit	No limit	No limit	No limit
Water content (mg/kg)	44	71	75	100	177
Test method and limits	EN ISO 12937 < 200	EN ISO 12937 < 200	EN ISO 12937 < 260	EN ISO 12937 < 290	EN ISO 12937 < 500
Ultimate					
C (wt%- mol. fr.)	84.34- 0.329	84.11- 0.333	83.28- 0.332	83.82- 0.340	76.93- 0.328
H (wt%- mol. fr.)	14.37- 0.668	14.01- 0.662	13.92- 0.664	13.52- 0.653	12.56- 0.639
N (wt%- mol. fr.)	< 0.5- 0.02	< 0.5- 0.02	< 0.5- 0.02	< 0.5- 0.02	< 0.5- 0.02
S (wt%- mol. fr.)	0.65- 0.001	0.55- 0.0008	0.57- 0.0009	0.54- 0.0008	< 0.5- 0.0008
K (µg/kg)	< 50	N/A	N/A	N/A	< 50
Test method and limits	EN 14108/ 14109	EN 14108/ 14109	EN 14108/ 14109	EN 14108/ 14109	EN 14108/ 14109
Na (µg/kg)	< 50	N/A	N/A	N/A	< 50
Ca (µg/kg)	< 0.5	N/A	N/A	N/A	< 0.5
Si (µg/kg)	< 0.5	N/A	N/A	N/A	< 0.5
Test method and limits	EN 14538 No limit	EN 14538 N/A	EN 14538 N/A	EN 14538 N/A	EN 14538 sum of K and Na < 5.0 mg/kg sum of Ca and Si < 5.0 mg/kg

Table 4. Results of ANOVA analysis

	D100/D100-CZA2		B10/B10-CZA2		B20/B20-CZA2		B30/B30-CZA2	
BSFC	*F*	*p*	*F*	*p*	*F*	*p*	*F*	*p*
Fuel	22.898	0.000	0738	0.399	0.087	0.771	39.885	0.000
Load	16.593	0.000	24.038	0.000	81.862	0.000	391.918	0.000
Fuel×Load	0.378	0.822	0.291	0.881	4.400	0.008	2.579	0.080
BTE (%)	*F*	*p*	*F*	*p*	*F*	*p*	*F*	*p*
Fuel	17.920	0.000	0.625	0.437	1.168	0.290	152.244	0.000
Load	4.975	0.004	8.202	0.000	53.954	0.000	647.937	0.000
Fuel×Load	0.643	0.636	0.323	0.860	3.643	0.018	10.837	0.000
HC	*F*	*p*	*F*	*p*	*F*	*p*	*F*	*p*
Fuel	21.124	0.000	5.619	0.026	12.311	0.002	0.132	0.721
Load	6.513	0.001	0.457	0.767	9.908	0.000	5.118	0.008
Fuel×Load	8.291	0.000	3.355	0.026	3.627	0.018	6.012	0.004
CO	*F*	*p*	*F*	*p*	*F*	*p*	*F*	*p*
Fuel	3.445	0.073	1.250	0.274	0.789	0.383	0.186	0.672
Load	0.526	0.717	3.954	0.013	7.176	0.001	19.138	0.000
Fuel×Load	1.536	0.217	1.888	0.144	7.942	0.000	8.462	0.001
CO_2	*F*	*p*	*F*	*p*	*F*	*p*	*F*	*p*
Fuel	4.615	0.040	0.111	0.742	1.461	0.238	25.007	0.000
Load	9.101	0.000	5.526	0.002	10.562	0.000	32.985	0.000
Fuel×Load	6.732	0.001	2.259	0.091	7.369	0.000	10.346	0.000
NOx	*F*	*p*	*F*	*p*	*F*	*p*	*F*	*p*
Fuel	1.478	0.234	0.477	0.496	0.060	0.808	20.461	0.000
Load	8.820	0.000	16.856	0.000	6.958	0.001	29.876	0.000
Fuel×Load	0.450	0.772	0.726	0.583	2.312	0.086	7.633	0.001

Figure
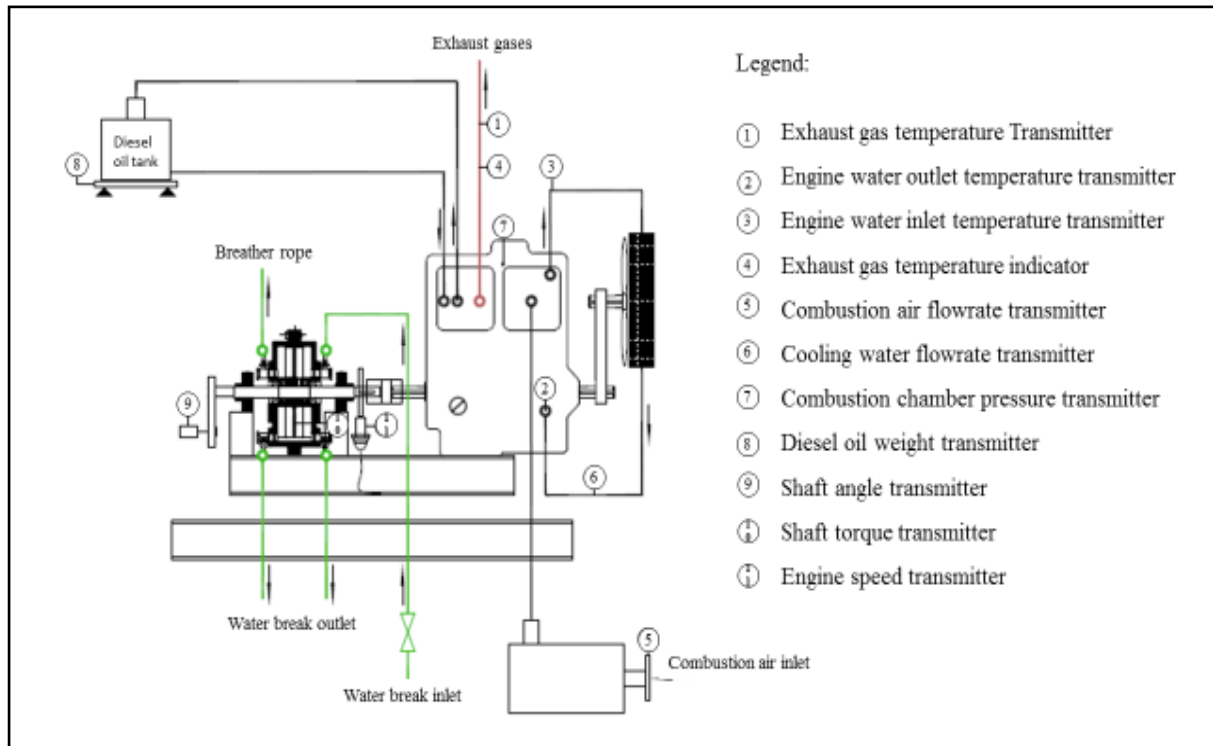
Fig. 1. Schematic diagram of engine test rig.
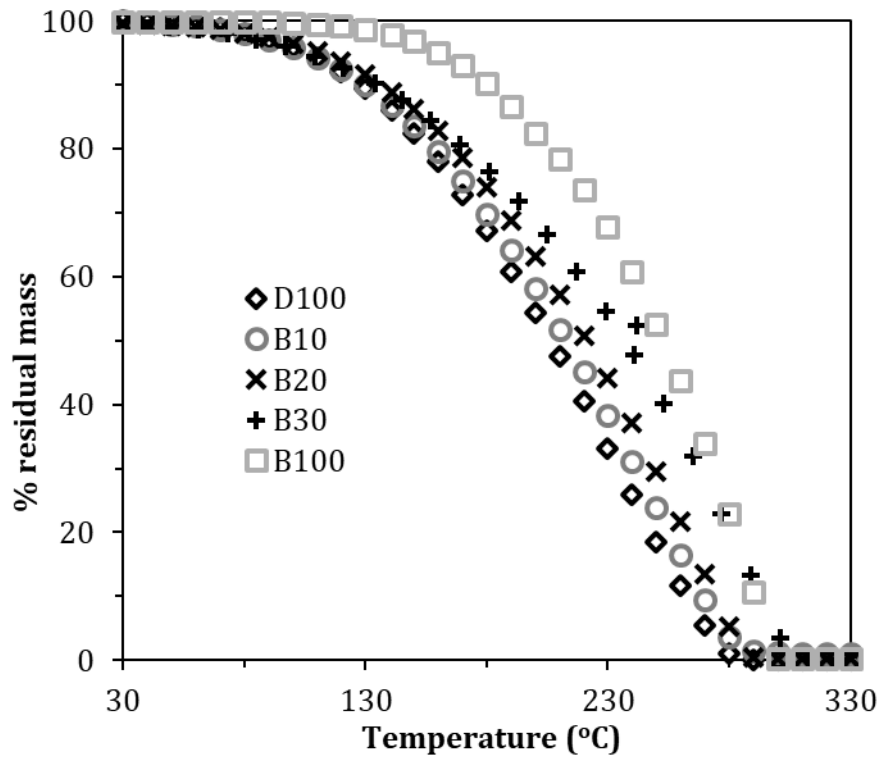
(a1)
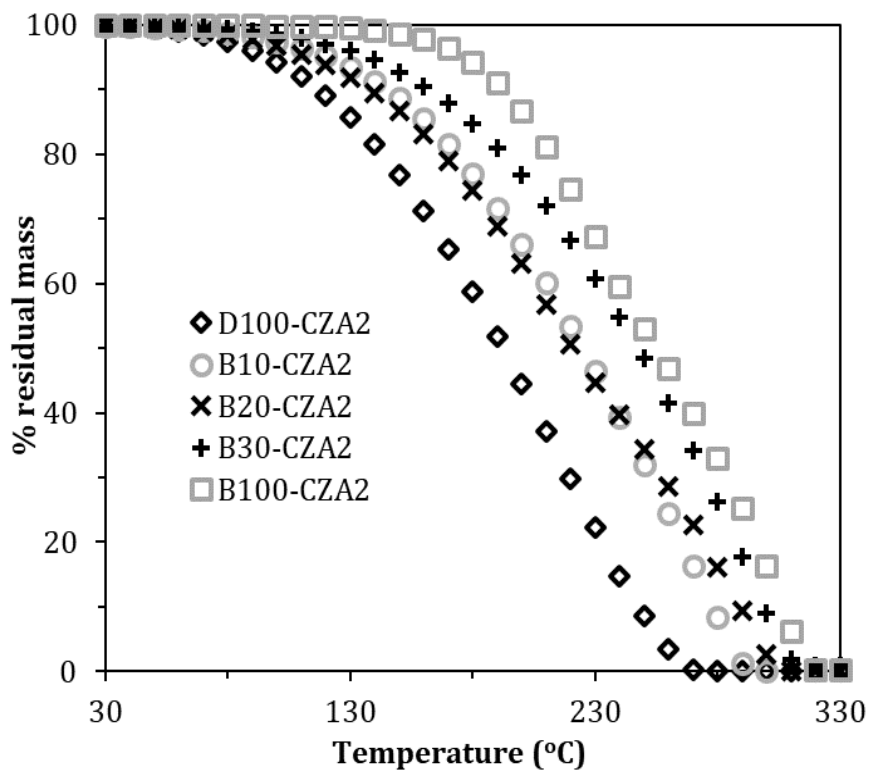
(a2)
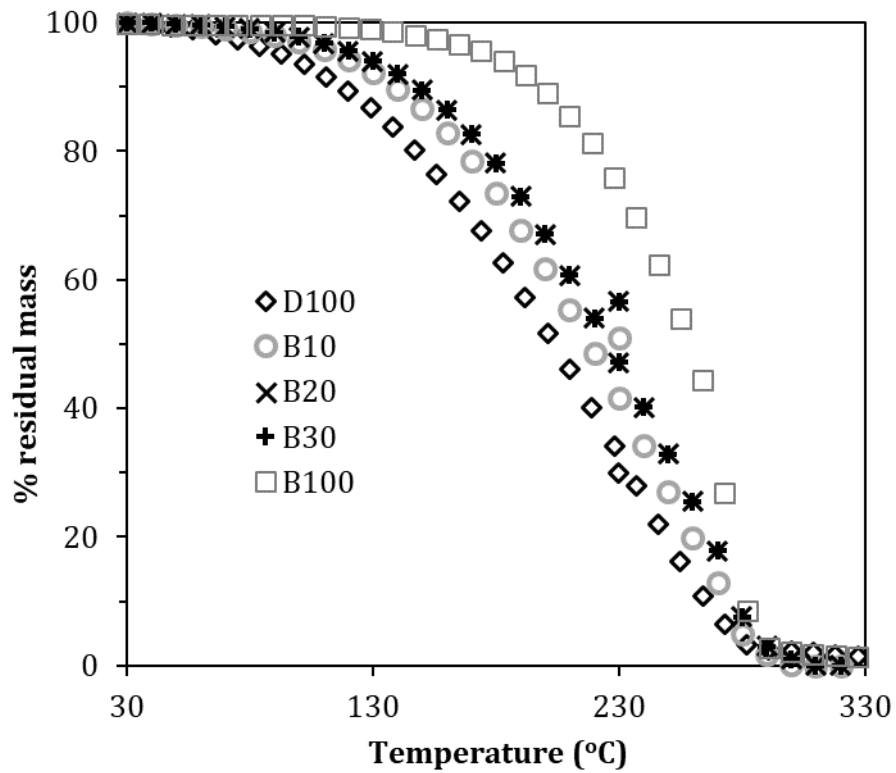
(b1)
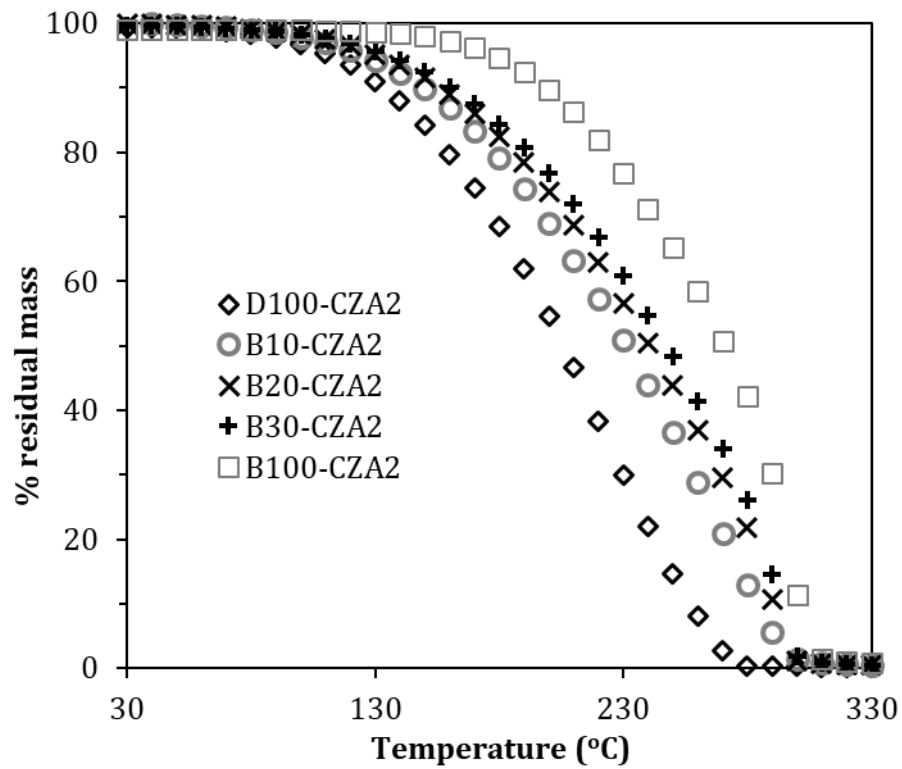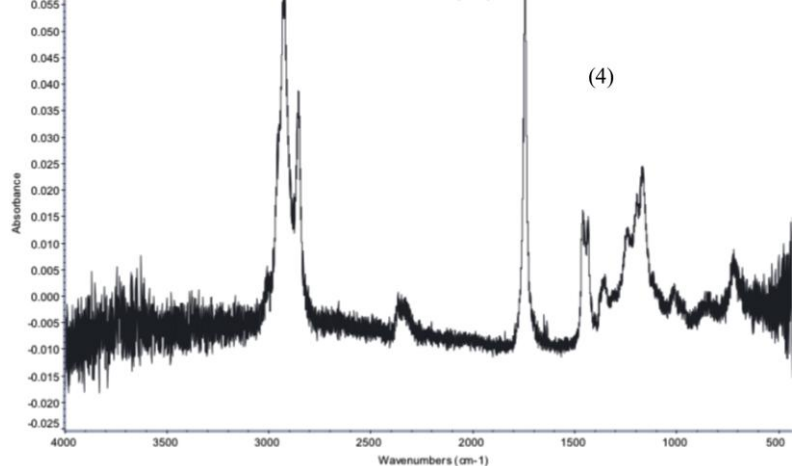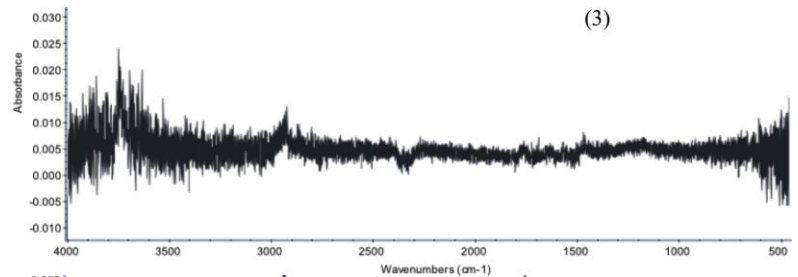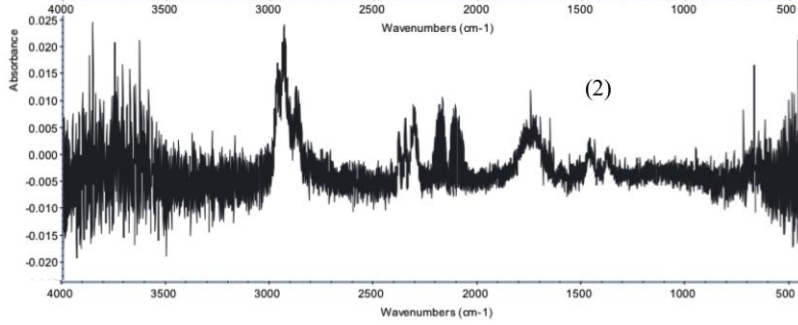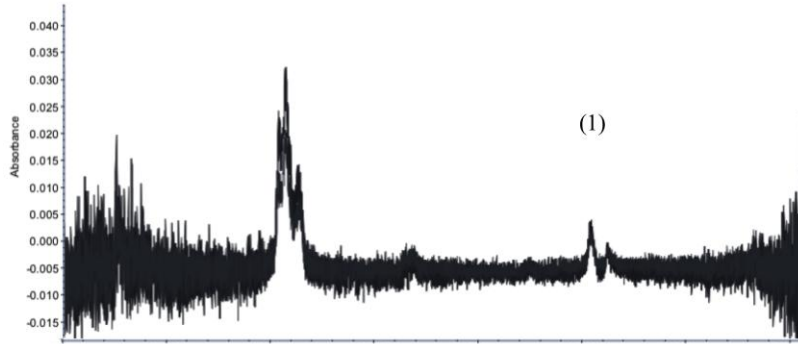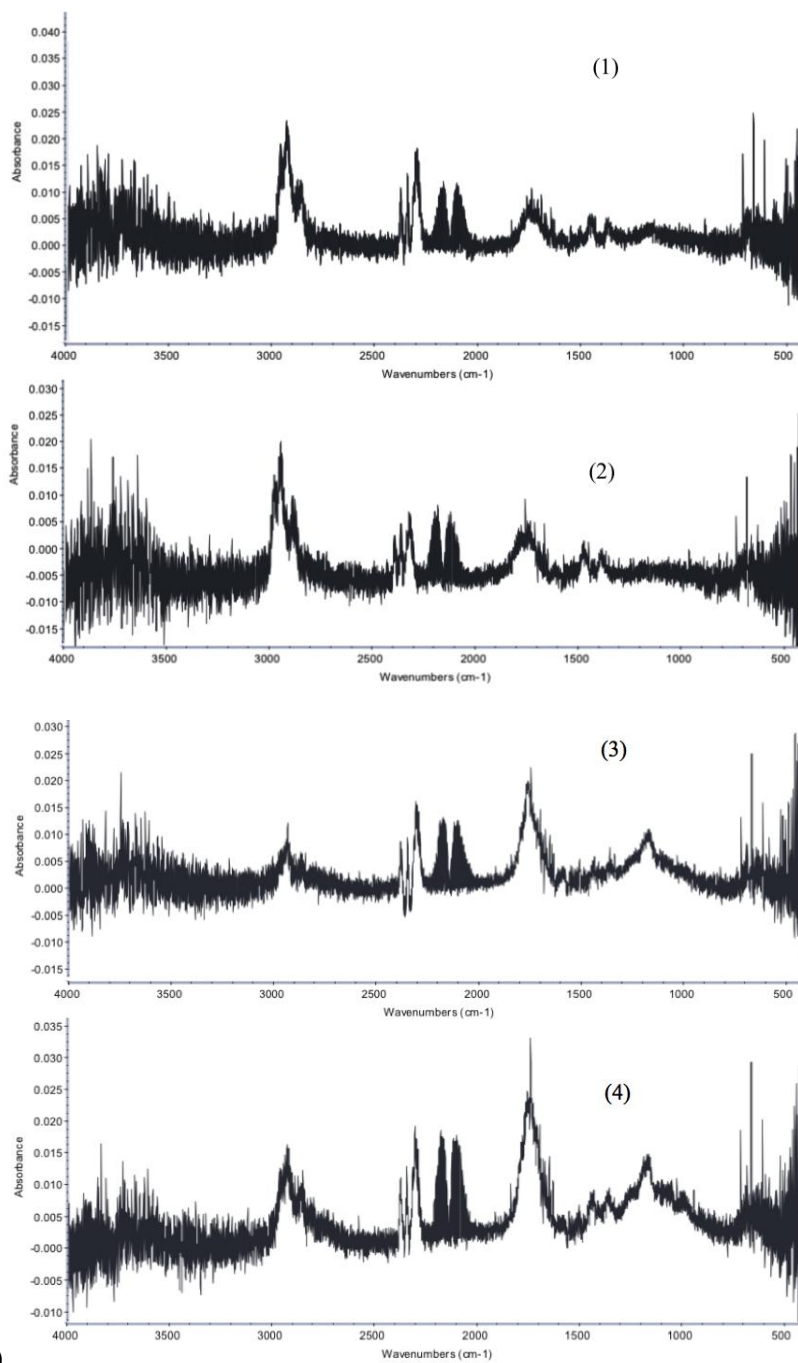

(b2)

Fig. 2. TGA (a) pyrolysis and (b) oxidation curves of D100, B10, B20, B30 and B100 at heating rate, $\beta = 10^{o}$C/min, without (1) and with the CZA2 dispersion (2).

(1)

(2)

(3)

(4)

(a)

4

Fig. 3. FTIR spectra at 150°C under (a) pyrolysis and (b) oxidation conditions of (1) D100, (2) D100-CZA2, (3) B100, and (4) B100-CZA2.
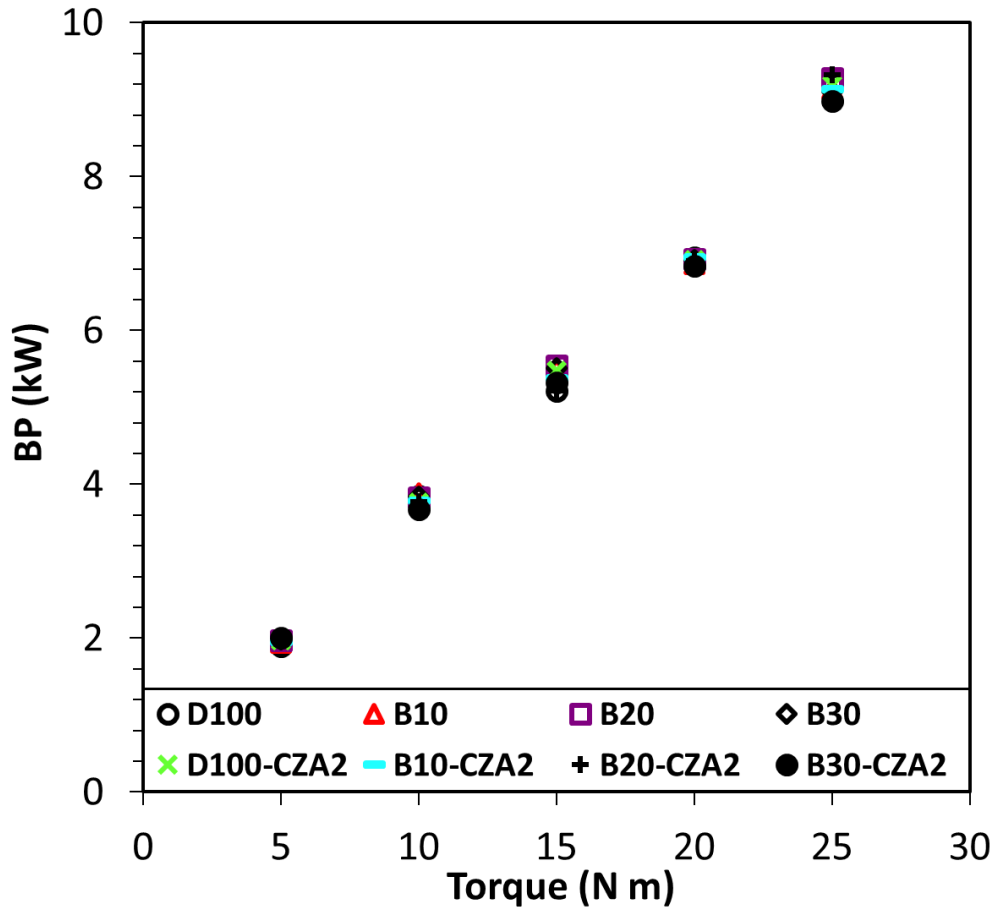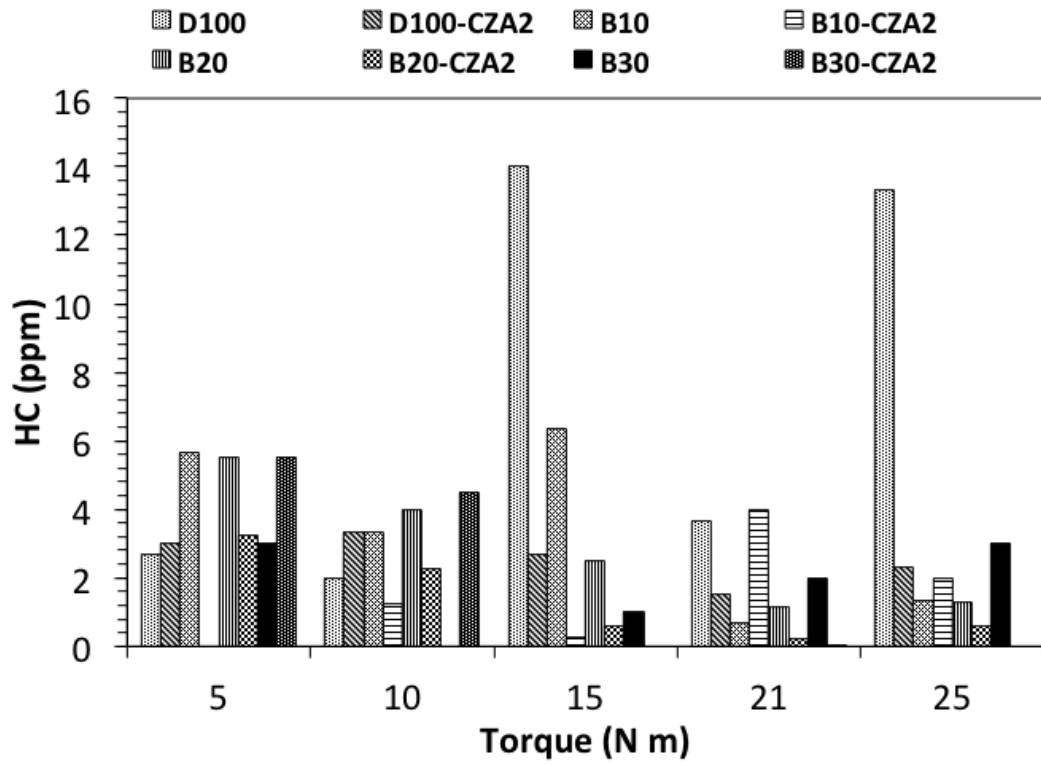
Fig. 4. Brake power (BP) of all tested fuels without and with the CZA2, at variable load conditions.
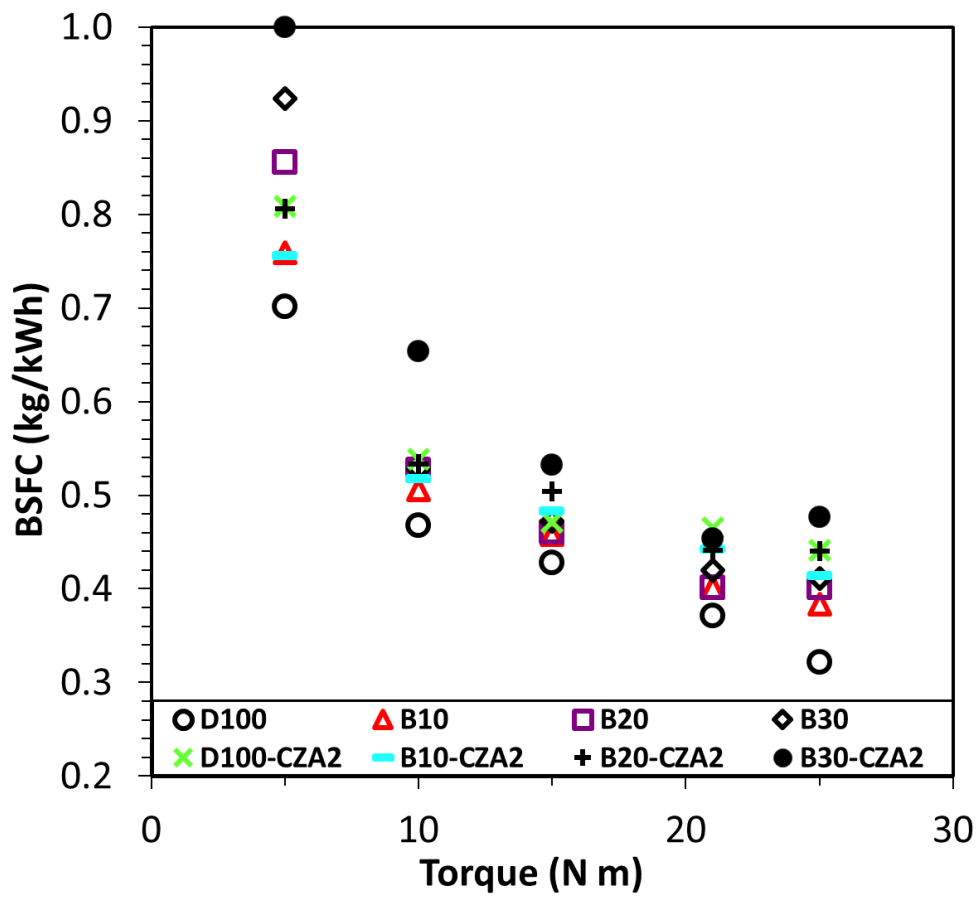
Fig. 5. Brake specific fuel consumption (BSFC) of all tested fuels without and with the CZA2, at variable load conditions.
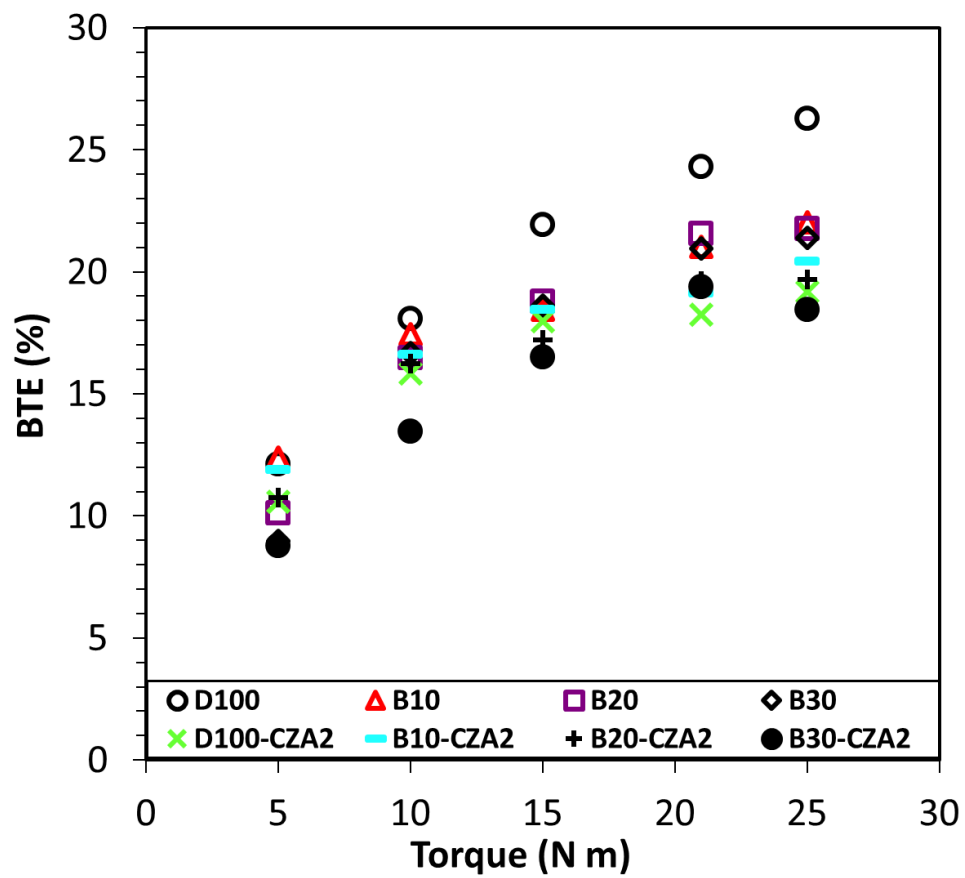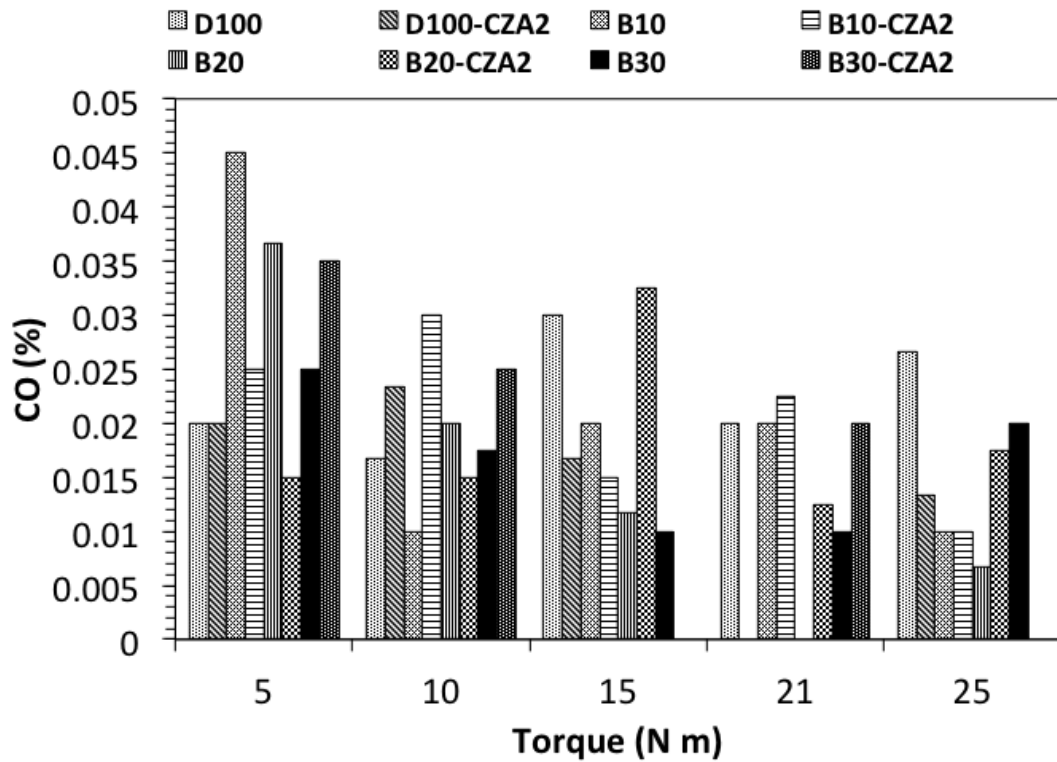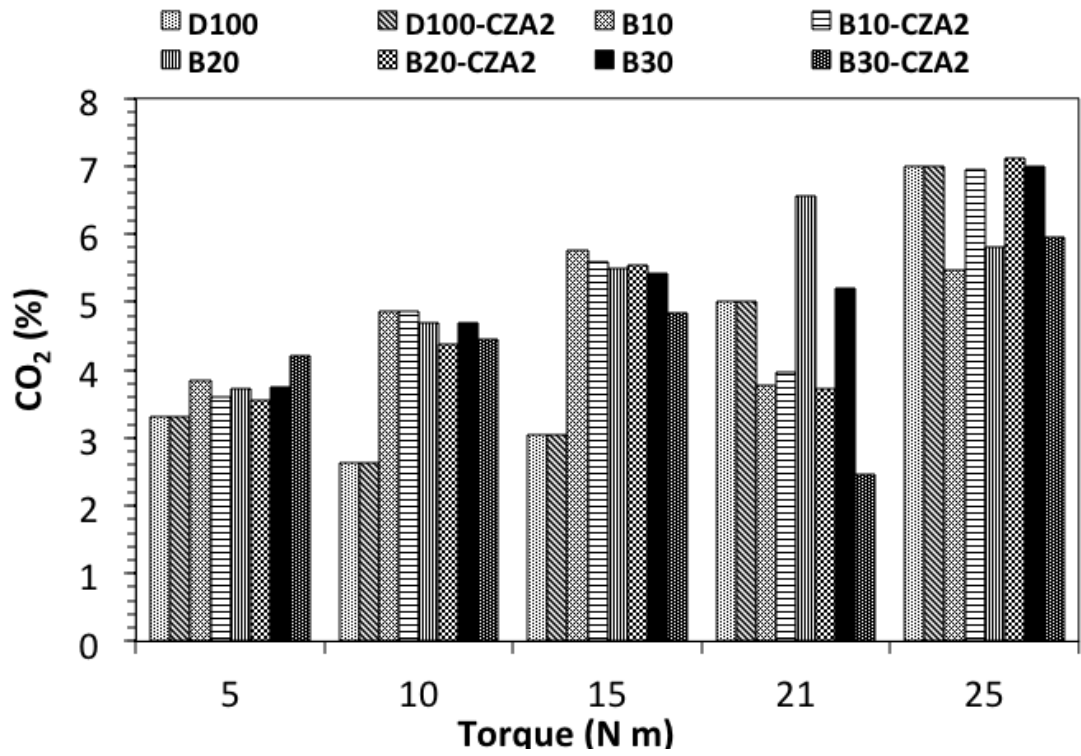
Fig. 6. Brake thermal efficiency (BTE) of all tested fuels without and with CZA2 at variable load conditions.
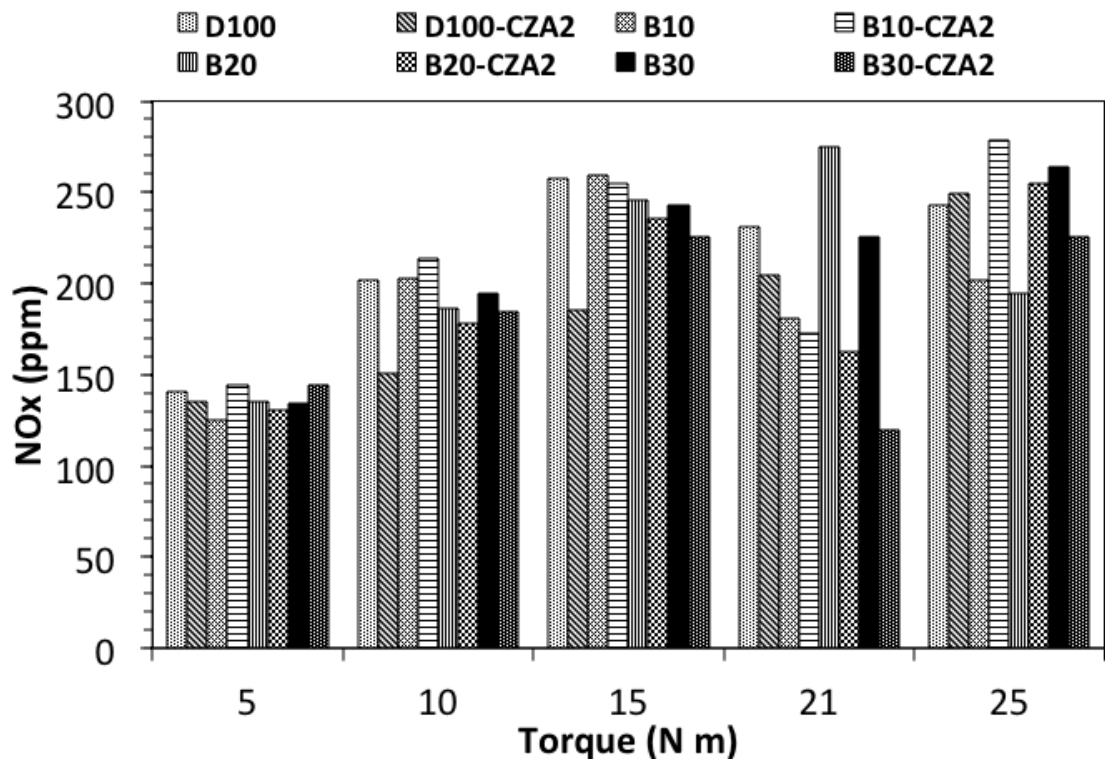
(a)

(b)

(c)

(d)

Fig. 7. (a) Unburned hydrocarbon (HC), (b) carbon monoxide (CO), (c) carbon dioxide (CO_2) and (d) nitrogen oxide (NOx) emissions of all tested fuels without and with CZA2 at variable load conditions.